High-quality, large-area monolayer graphene for efficient bulk laser mode-locking near 1.25 μm

Won Bae Cho,[1] Jun Wan Kim,[1] Hwang Woon Lee,[1] Sukang Bae,[2] Byung Hee Hong,[2] Sun Young Choi,[1] In Hyung Baek,[1] Kihong Kim,[1] Dong-Il Yeom,[1] and Fabian Rotermund[1,*]

[1]*Department of Physics & Division of Energy Systems Research, Ajou University, San 5 Wonchun, Suwon 443-749, South Korea*

[2]*Department of Chemistry & SKKU Advanced Institute of Nanotechnology (SAINT), Sungkyunkwan University, Suwon 440-746, South Korea*

**Corresponding author: rotermun@ajou.ac.kr*

Received August 4, 2011; revised September 8, 2011; accepted September 8, 2011; posted September 9, 2011 (Doc. ID 152402); published October 14, 2011

High-quality monolayer graphene as large as $1.2 \times 1.2\,\mathrm{cm}^2$ was synthesized by chemical vapor deposition and used as a transmitting saturable absorber for efficient passive mode-locking of a femtosecond bulk solid-state laser. The monolayer graphene mode-locked Cr:forsterite laser was tunable around 1.25 μm and delivered sub-100 fs pulses with output powers up to 230 mW. The nonlinear optical characteristics of the monolayer graphene saturable absorber and the mode-locked operation were then compared with the case of the bilayer graphene saturable absorber.

OCIS codes: 140.4050, 140.3580, 160.4236, 160.4330.

Low-dimensional carbon nanostructures such as carbon nanotubes (CNTs) and graphene have been widely investigated for optoelectronic and photonic applications due to their unique characteristics [1,2]. In particular, single-walled CNTs (SWCNTs) turned out to be very promising nonlinear saturable absorber materials for ultrafast laser mode-locking. Recently, by utilizing the nonlinear absorption in E_{11} and E_{22} electronic transitions of semiconducting SWCNTs, passive mode-locking of fiber and bulk solid-state lasers has been successfully demonstrated at different wavelengths between 800 nm and 2.0 μm [2–6]. As another alternative, graphene, i.e. a two-dimensional lattice of carbon atoms arranged in a hexagonal structure, is newly suggested as a suitable material for broadband saturable absorption. Two distinct carrier relaxations of ~100 fs and <2 ps, associated with carrier-carrier intraband scattering and electron-hole interband recombination processes, respectively, were reported in the previous time-resolved spectroscopic investigation at 780 nm [7]. Graphene is a point-bandgap semiconductor with a linear energy dispersion of Dirac electrons that enables the use of it as ultrafast saturable absorbers applicable in the ultrabroad spectral range without bandgap engineering, while the spectral applicability of SWCNT-SAs is limited by diameters and chiralities of currently available SWCNTs.

Most previous investigations on laser mode-locking employing graphene-based saturable absorbers (graphene SAs) were focused on fiber lasers near 1.0 and 1.5 μm, including the first demonstration [2], where graphene layers of not well-defined layer numbers, graphene/polymer composites, and graphene flakes produced by liquid-phase exfoliation, mechanical exfoliation, or chemical vapor deposition (CVD) methods were mostly used as the mode-locker after transferring them onto fiber pigtails [2,8,9]. In those cases, the output powers were limited in the level of 1 mW or even lower and the linear and nonsaturable losses were quite large, not applicable for bulk lasers. There are two previous demonstrations on bulk laser mode-locking using graphene SAs, where ceramic Nd:YAG and bulk Nd:$GdVO_4$ crystal served as the gain media [10,11]. The generated pulses near 1 μm were about 4–16 ps long and the insertion loss in the laser cavity seems to be still too high for a stable bulk laser mode-locking. Recently, we reported for the first time the applicability of monolayer graphene as a mode-locker for femtosecond bulk solid-state lasers [12]. In this Letter, we present the fabrication of high-quality monolayer and bilayer graphene SAs and their nonlinear optical characteristics such as nonlinear transmission and response behaviors. The monolayer graphene SA mode-locked bulk laser operating near 1.25 μm enables us to deliver stable 94 fs pulses with average output powers up to 230 mW at a repetition rate of 75 MHz. Note that the widespread mode-locking devices such as semiconductor saturable absorber mirrors (SESAMs) for this wavelength have not been well developed to a mature level, except for some initial demonstrations.

A similar technique reported in [13] was applied for growing high-quality, large-area graphene films. The monolayer graphene was synthesized by CVD of the mixture of methane and hydrogen gases on Cu foils at 1000 °C. After spin-coating the well-grown graphene monolayer with 5 wt.% polymethyl-methacrylate (PMMA) in chlorobenzene, the underlying Cu foil was etched by 0.5 M aqueous $FeCl_3$ solution. Subsequently, the graphene layer supported by PMMA was transferred onto a 1 in. quartz substrate without any intense mechanical and chemical treatments and dried on a hot plate at 80 °C. Finally, acetone was used to remove the PMMA layer. The measured Raman spectra show that the transferred graphene film consists of >95% monolayer. Furthermore, a layer-by-layer stacking of monolayer graphene enables a defined increase in the number of layers. Figure 1 shows the linear transmission of the monolayer and bilayer graphene with photographic images of both transmitting graphene SAs (inset). The size of the graphene layer transferred onto the substrate was $>1.2 \times 1.2\,\mathrm{cm}^2$.

The linear transmission of the monolayer graphene around 1.25 μm was measured to be 97.6%, which nearly approaches the theoretical value given by

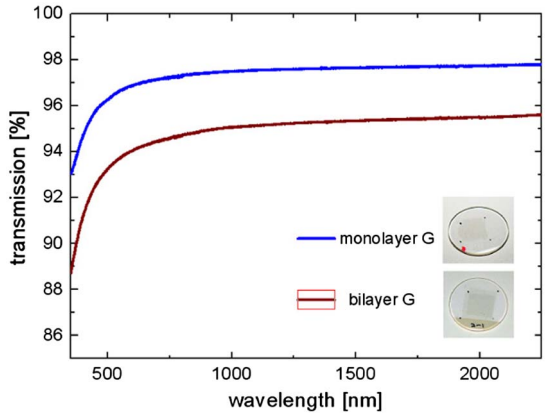

Fig. 1. (Color online) Linear transmission of monolayer and bilayer graphene and photographic images of SAs (inset).

$T \approx 1 - \pi\alpha \approx 97.7\%$ and therefore indicates its high quality. Here, α denotes the fine-structure constant [14]. For multilayer graphene, the absorption loss is given by an integer multiple of 2.3% per additional layer. It agrees well with the measured transmission of our bilayer graphene sample shown in Fig. 1.

The nonlinear response dynamics of the graphene SAs were investigated at 1.25 μm by time-resolved pump-probe measurements using a near-infrared optical parametric oscillator (Coherent Inc. Mira OPO) delivering 160 fs pulses. The measured pump-probe trace in the monolayer graphene SA (Fig. 2) indicates a biexponential decay of saturable absorption with an instantaneous response of 155 fs with a slow $1/e$ recovery time of 1.45 ps. The bilayer graphene SA shows a similar behavior.

The fast decay is associated with carrier-carrier intraband collision and phonon emission and the slow component is known to be caused by electron-hole interband relaxation and cooling of hot phonons [15]. The response time constants are comparable to those of SESAMs and SWCNT-SAs [16,17].

To estimate parameters important for mode-locking, such as saturation fluences (F_{sat}), modulation depths (ΔT) and nonsaturable losses, nonlinear transmission measurements were performed in the monolayer and bilayer graphene SAs at 1.25 μm. The measured fluence-dependent transmission changes are shown in the inset of Fig. 2. From the fit to the data, we extracted $\Delta T \approx 0.54$ and 1.30%, $F_{\mathrm{sat}} \approx 14.5$ and 22.5 μJ/cm^2, and nonsaturable losses of 1.61 and 3.05% for the monolayer and bilayer graphene SAs, respectively. These values are well-suited to achieve stable mode-locking of typical bulk lasers.

For passive mode-locking of a bulk laser employing graphene SAs, we used a similar Cr:forsterite laser used previously for SWCNT-SA mode-locking experiment [16]. A Brewster-cut, 11 mm long Cr:forsterite crystal was placed in an astigmatically compensated x-cavity between two folding mirrors with a radius of curvature (ROC) of −100 mm and pumped by a cw Yb:fiber laser (IPG Photonics) at 1064 nm. Two highly reflecting mirrors with the same ROC additionally formed the second cavity in the longer arm and the graphene SA was placed near the focus in this cavity. Depending on the absorber position the beam size ω_0 on the absorber could be varied between 40 and 80 μm. Without dispersion compensation, the monolayer graphene SA mode-locked Cr:forsterite laser produced stable 7.2 ps pulses with a spectral bandwidth of 3.6 nm at 1.24 μm. The maximum output power was 260 mW. For dispersion compensation, a SF10 prism pair was inserted in the resonator arm containing the output coupler (OC). Characteristics of the output pulses in the femtosecond mode-locked regime were investigated with three OCs of different transmissions of 3.3%, 5%, and 7% (Fig. 3). Average output powers up to 230 mW were achieved at 75 MHz with the 5% OC. In all cases, the laser was easily mode-locked or self-starting in a wide power range without appearance of multiple pulsing and Q-switching instabilities. The uniformity of the SA was verified by changing the absorber position.

The mode-locked operation was stable for hours and no visible damages on the absorber were observed. At higher output than 230 mW, multiple pulsing and cw components strongly appeared and interrupted mode-locking. Employing the bilayer graphene SA, the mode-locked laser with 5% OC delivered a maximum output power of 113 mW. Lower power and higher lasing and mode-locking thresholds in this case were due to the increased insertion loss through the doubled layer number.

The pulse duration was measured by the intensity autocorrelation technique. Figure 4 shows the optical spectra and the autocorrelation trace (inset). The mode-locked Cr:forsterite laser could be tuned across the wavelength

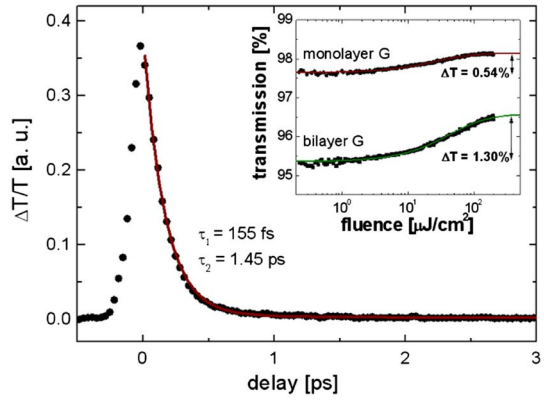

Fig. 2. (Color online) Pump-probe trace of the monolayer graphene SA and nonlinear transmission measurements in the monolayer and bilayer graphene SAs (inset).

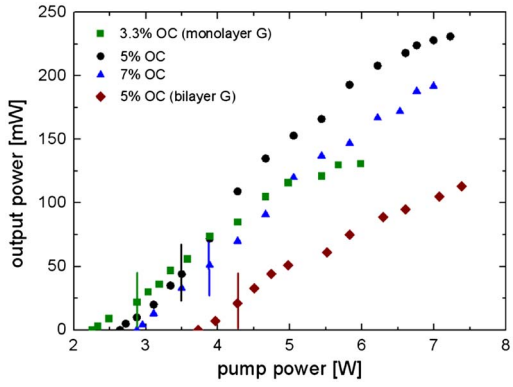

Fig. 3. (Color online) Output powers from the monolayer graphene SA mode-locked Cr:forsterite laser for different OCs. Solid vertical lines denote the mode-locking threshold for each OC.

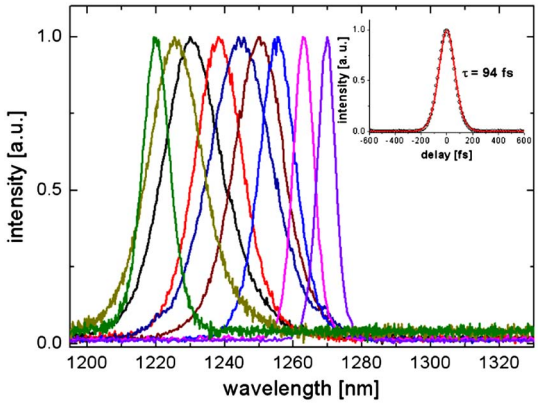

Fig. 4. (Color online) Tunable laser spectra from the monolayer graphene SA mode-locked Cr:forsterite laser and the autocorrelation trace (inset).

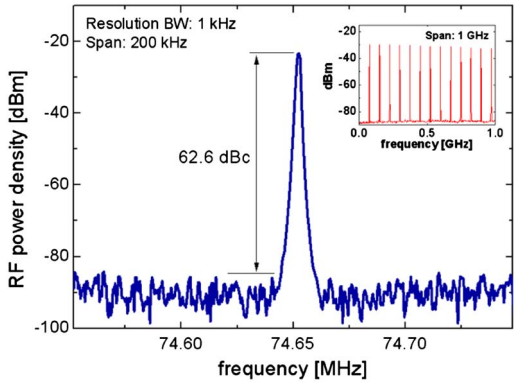

Fig. 5. (Color online) RF spectrum of the fundamental beat note and 1 GHz span of the spectrum (inset).

from 1.22 to 1.27 μm by adjusting the second prism and a knife inserted in front of OC. Narrower optical spectra at the edge of the tuning range were caused by the limited bandwidth of the dielectric coating of the mirrors used.

Assumption of sech^2-pulse shapes indicates a pulse duration of 94 fs in the monolayer graphene SA mode-locked operation. The corresponding spectrum near 1.24 μm with a 20 nm bandwidth leads to a time-bandwidth product of 0.37, close to Fourier limit. To verify mode-locking stability, radio-frequency (RF) spectra were recorded in different spans (Fig. 5). The first intermode beat at 74.65 MHz, measured with a resolution bandwidth of 1 kHz, displayed a pedestal peak separation of 62.6 dB above carrier. The inset of Fig. 5 shows a 1 GHz wide-span measurement of the signal. The RF spectrum with a high extinction ratio clearly shows the absence of any kind of multiple pulsing and Q-switching instabilities.

In conclusion, high-quality, large-area graphene SAs were successfully fabricated and used for efficient bulk solid-state laser mode-locking. The monolayer graphene SA mode-locked Cr:forsterite laser was tunable around 1.25 μm and delivered stable sub-100 fs pulses with 230 mW average power at 75 MHz. Because of unique band structure and superior nonlinear optical properties, monolayer graphene can be further applied for other bulk lasers in the wide spectral region. Another additional advantage of graphene-based SAs is that the modulation depth can be easily varied by layer-by-layer stacking of graphene layer.

This work was supported by the National Research Foundation (NRF) grants funded by the Korean Government, Ministry of Education, Science, and Technology (MEST) (2011-0017494 and 2011-0001054). S. Bae and B. H. Hong also acknowledge financial support from the NRF funded by MEST (2011-0017587).

References

1. F. Bonaccorso, Z. Sun, T. Hasan, and A. C. Ferrari, Nat. Photon. **4**, 611 (2010).
2. T. Hasan, Z. Sun, F. Wang, F. Bonaccorso, P. H. Tan, A. G. Rozhin, and A. C. Ferrari, Adv. Mater. **21**, 3874 (2009).
3. S. Y. Set, H. Yaguchi, Y. Tanaka, and M. Jablonski, J. Lightwave Technol. **22**, 51 (2004).
4. W. B. Cho, J. H. Yim, S. Y. Choi, S. Lee, A. Schmidt, G. Steinmeyer, U. Griebner, V. Petrov, D.-I. Yeom, K. Kim, and F. Rotermund, Adv. Funct. Mater. **20**, 1937 (2010).
5. I. H. Baek, S. Y. Choi, H. W. Lee, W. B. Cho, V. Petrov, A. Agnesi, V. Pasiskevicius, D.-I. Yeom, K. Kim, and F. Rotermund, Opt. Express **19**, 7833 (2011).
6. W. B. Cho, A. Schmidt, J. H. Yim, S. Y. Choi, S. Lee, F. Rotermund, U. Griebner, G. Steinmeyer, V. Petrov, X. Mateos, M. C. Pujol, J. J. Carvajal, M. Aguiló, and F. Díaz, Opt. Express **17**, 11007 (2009).
7. J. M. Dawlaty, S. Shivaraman, M. Chandrashekhar, F. Rana, and M. G. Spencer, Appl. Phys. Lett. **92**, 042116 (2008).
8. Z. Sun, T. Hasan, F. Torrisi, D. Popa, G. Privitera, F. Wang, F. Bonaccorso, D. M. Basko, and A. Ferrari, ACS Nano **4**, 803 (2010).
9. Y. M. Chang, H. Kim, J. H. Lee, and Y.-W. Song, Appl. Phys. Lett. **97**, 211102 (2010).
10. W. D. Tan, C. Y. Su, R. J. Knize, G. Q. Xie, L. J. Li, and D. Y. Tang, Appl. Phys. Lett. **96**, 031106 (2010).
11. J.-L. Xu, X.-L. Li, Y.-Z. Wu, X.-P. Hao, J.-L. He, and K.-J. Yang, Opt. Lett. **36**, 2011 (2011).
12. W. B. Cho, H. W. Lee, S. Y. Choi, J. W. Kim, D.-I. Yeom, F. Rotermund, J. Kim, and B. H. Hong, in *Conference on Lasers and Electro-Optics*, OSA Technical Digest (2010), paper JThE86.
13. K. S. Kim, Y. Zhao, H. Jang, S. Y. Lee, J. M. Kim, K. S. Kim, J.-H. Ahn, P. Kim, J.-Y. Choi, and B. H. Hong, Nature **457**, 706 (2009).
14. R. R. Nair, P. Blake, A. N. Grigorenko, K. S. Novoselov, T. J. Booth, T. Stauber, N. M. R. Peres, and A. K. Geim, Science **320**, 1308 (2008).
15. T. Kampfrath, L. Perfetti, F. Schapper, C. Frischkorn, and M. Wolf, Phys. Rev. Lett. **95**, 187403 (2005).
16. W. B. Cho, J. H. Yim, S. Y. Choi, S. Lee, U. Griebner, V. Petrov, and F. Rotermund, Opt. Lett. **33**, 2449 (2008).
17. U. Keller, K. J. Weingarten, F. X. Kärtner, D. Kopf, B. Braun, I. D. Jung, R. Fluck, C. Hönninger, N. Matuschek, and J. Aus der Au, IEEE J. Sel. Top. Quantum Electron. **2**, 435 (1996).